ChemComm

Accepted Manuscript

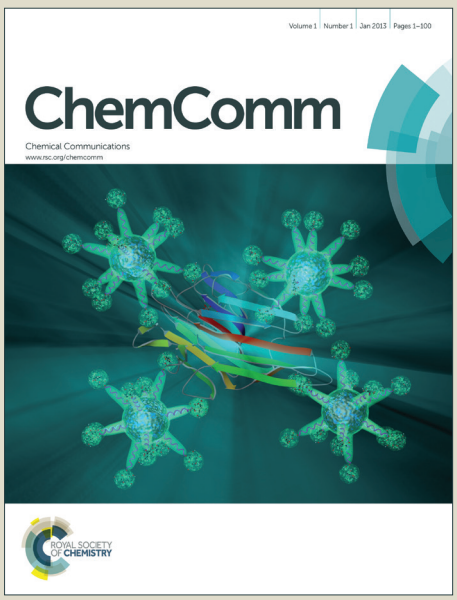

ROYAL SOCIETY OF CHEMISTRY

www.rsc.org/chemcomm

Cite this: DOI: 10.1039/c0xx00000x

www.rsc.org/xxxxxx

ARTICLE TYPE

Electrodeposition of PbO and In Situ Conversion to $CH_3NH_3PbI_3$ for Mesoscopic Perovskite Solar Cells

Xue-Ping Cui,[a,b] Ke-Jian Jiang,[a,*] Jin-Hua Huang,[a] Xue-Qin Zhou,[b,*] Mei-Ju Su,[a,b] Shao-Gang Li,[a] Qian-Qian Zhang,[a,b] Lian-Min Yang,[a] Yan-Lin Song [a,*]

Received (in XXX, XXX) Xth XXXXXXXXX 20XX, Accepted Xth XXXXXXXXX 20XX

DOI: 10.1039/b000000x

The perovskite $CH_3NH_3PbI_3$ was prepared on a mesoscopic TiO_2 film, starting from electrodepositing PbO, to iodination for PbI_2, then interdiffusion reaction with CH_3NH_3I. The as-prepared film was used as a light absorber for the perovskite solar cells, exhibiting a high PCE of 12.5% under standard AM 1.5 conditions.

Evolving from the dye-sensitized solar cells, organic-inorganic hybrid perovskite materials such as $CH_3NH_3PbX_3$ (X=Cl, Br, I) have attracted great attention as light absorbers in efficient photovoltaic cells since the first report by Miyasaka group in 2009.[1-12] The perovskite active materials can be deposited from the precursor solutions at low temperatures, possessing most of the properties required for the low-cost and high efficient solar cells: desired direct band gap, high absorption coefficient, low fundamental energy losses, large bipolar transport mobility and long carrier diffusion lengths.[13,14] These properties enabled feasible construction of mesoscopic or planar structured devices with various architectures, having power conversion efficiencies (PCEs) ranging from 8% to 16%.[1-12]

In the mesoscopic solar cells, the perovskite materials were usually deposited in mesoporous metal oxide scaffolds, typically TiO_2 and Al_2O_3, through spin coating technique. In early stage, one-step spin coating method was employed to directly deposit the perovskite materials from a mixture of PbI_2 and CH_3NH_3I in a polar solvent, delivering a power conversion efficiency of 10%. However, effective infiltration of the perovskite within the mesoscopic film is a challenge. The resulting devices usually display a wide spread of photovoltaic performance due to the difficulty to control the morphology over the whole deposited area.[7,15,16] Following that, a sequential deposition method, originally developed by Mitzi *et al.*, was employed for the formation of the crystalline perovskite within the porous films.[17] In this method, high concentrated PbI_2 solution was first infiltrated at elevated temperatures into the films, and then the PbI_2 was in situ transferred to the high crystalline perovskite in the porous film through the solid-liquid intercalation reaction in a CH_3NH_3I solution. With the method, a large amount of PbI_2 was confined within the film to ensure sufficient loading of perovskite materials on the porous film for highly efficient light harvesting, which is responsible for the high conversion efficiency of 15%.[7] In both the cases, however, the challenge is to fully fill the pores with the perovskite materials without leaving voids for the sufficient light harvesting. In this case, the naked TiO_2 surface with no perovskite coverage could directly make contact with hole-transport layer or electrode, and result in serious back charge transfer, leading to poor open-circuit voltage and thus low device performance. Thus, the desirable deposition technique is of crucial importance with effective filling of the perovskite in the porous film for highly efficient mesoscopic solar cells.

Electrochemical deposition is a versatile technique for producing surface coatings, owing to its precise controllability, room temperature operation, rapid deposition rate, and relatively low cost. More importantly, electrodeposition can provide superior coverage to relatively inaccessible surfaces of the substrate, especially for the coating in the mesoporous scaffold films.[18-20] Here, we report a facile and efficient method for the fabrication of the perovskite in the mesoscopic TiO_2 film. As schematically illustrated in **Scheme 1**. PbO is first electrochemically deposited within the TiO_2 film, followed by in-situ transformed to PbI_2 by iodization and finally converted to $CH_3NH_3PbI_3$ by interdiffusion reaction with CH_3NH_3I. Using this technique, the perovskite $CH_3NH_3PbI_3$ was fully filled in the porous TiO_2 film with a dense and flat perovskite upper layer on the surface. The resultant solar cells yielded a power conversion efficiency of 12.5% under standard AM 1.5 conditions. The technique is environmentally sound for the production of the perovskite mesoscopic solar cells at large scale.

Electrodeposition of metal oxide films is usually conducted by cathodic reactions in the aqueous solutions. The formation mechanism of the metal oxide films was postulated as follows: OH^- ions generated in cathode react with metal cation, such as Pb^{2+}, to form corresponding metal oxide PbO or metal hydroxide $Pb(OH)_2$ (Eq.1 and 2). The later can be converted to PbO after dehydration.[19,21]

$$Pb^{2+} + 2\,OH^- \longrightarrow PbO + H_2O \quad (1)$$

$$Pb^{2+} + 2\,OH^- \longrightarrow Pb(OH)_2 \quad (2)$$

$$Pb(OH)_2 \longrightarrow PbO + H_2O \quad (3)$$

Here, the PbO electrodeposition was carried out in a single-compartment cell, where the mesoporous TiO_2 coated - FTO-glass was used as a working electrode, a Pt wire as a counter

electrode. The deposition baths consisted aqueous solutions of 2 mM $Pb(NO_3)_2$ and 0.2 M H_2O_2. The experiment details can be found in the Supporting Information. The freshly deposited film appears light yellow, indicating that PbO could be directly deposited in the conditions, and the reaction would be proceeded according to the Eq.1. The generated base in the reaction would come from the reduction of hydrogen peroxide rather than the reduction of nitrate ions at the low concentration of $Pb(NO_3)_2$.[21]

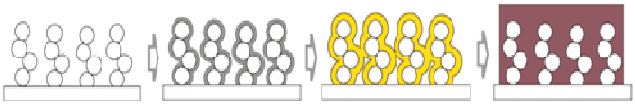

Scheme 1. Formation processes of the perovskite. on the mesoporous TiO_2 film, from electrodeposited PbO to PbI_2, then $CH_3NH_3PbI_3$.

After the electrodeposition, slight opaque yellow color was observed on the TiO_2 film, indicating the formation of PbO. The top-view and cross-sectional SEM images of the as-deposited PbO film are clearly different from those of the bare TiO_2 film (**Figure 1a ~ 1d**). It can be observed that the PbO was well filled in the pores of the TiO_2 film, as evidenced by the darker areas and the diminished contrast features in the TiO_2 layer. Interestingly, the film was covered with a layer of low-crystalline PbO, different from the high crystalline thin platelet PbO film deposited on ITO-substrate by eletrodeposition method.[19] In addition, EDX linescan for the cross sectional film of the PbO coated mesoscopic TiO_2 film was characterized, and the result showed that the electrodeposited PbO was well filled on the mesoscopic TiO_2 film, as shown in **Figure S1.**The as-prepared PbO film was exposed in iodine vapors with the active layer downwards in an enclosed dark glass chamber.[22] After iodination at 80°C for 20 minutes, the slight opaque yellow film became bright yellow and transparent. The film surface was fully covered by a layer of interconnected rice-shaped PbI_2 crystals, which is high crystalline with the grain sizes of 100-200 nm and the thickness of ~200 nm, as shown in **Figure 1e and 1f**. The formation of the upper layer of PbI_2 is probably due to the volume expansion from the interdiffusion reaction of the layered PbO and iodine vapors.[22] This upper layer is beneficial to the further formation of the perovskite for improving light harvesting capacity and thus the device performance, which is intensively expected in the sequential deposition for the perovskite mesoscopic solar cells.[7] For the formation of the perovskite, the PbI_2 film was deposited with a layer of methylammonium iodide (MAI) by spin coating technique, followed by the thermal annealing according to the interdiffusion methods.[23] After the interdiffusion reaction at 150 °C for 2 h under N_2 atmosphere, the dark brown perovskite was formed, as shown in **Figure 1g and 1h**, where the perovskite crystals were fully inlayed on the surface of the TiO_2 film with a dense and flat perovskite upper layer. As compared with the PbI_2 coated film, the grain size and the film thickness increase to 200~1000 nm and 350 nm, respectively, due to the volume expansion.[12] In **Figure.S2 and S3**, EDX patterns of the cross sectional PbI_2 and $CH_3NH_3PbI_3$ coated mesoscopic TiO_2 film showed that the atomic ratios for Pb and I are about 1:2 and 1:3 for PbI_2 and $CH_3NH_3PbI_3$, respectively, indicating that iodination for PbI_2, and interdiffusion reaction with MAI could be well processed. In addition, the formed PbI_2 film was also emerged in the MAI-2-propanol solution for the formation of the perovskite according to the reported dipping method.[17] Different from the former film, the dipping method gave highly crystallized perovskite crystals, which scattered on the TiO_2 film with a highly rough perovskite upper layer, as shown in **Figure S4** in supporting information.

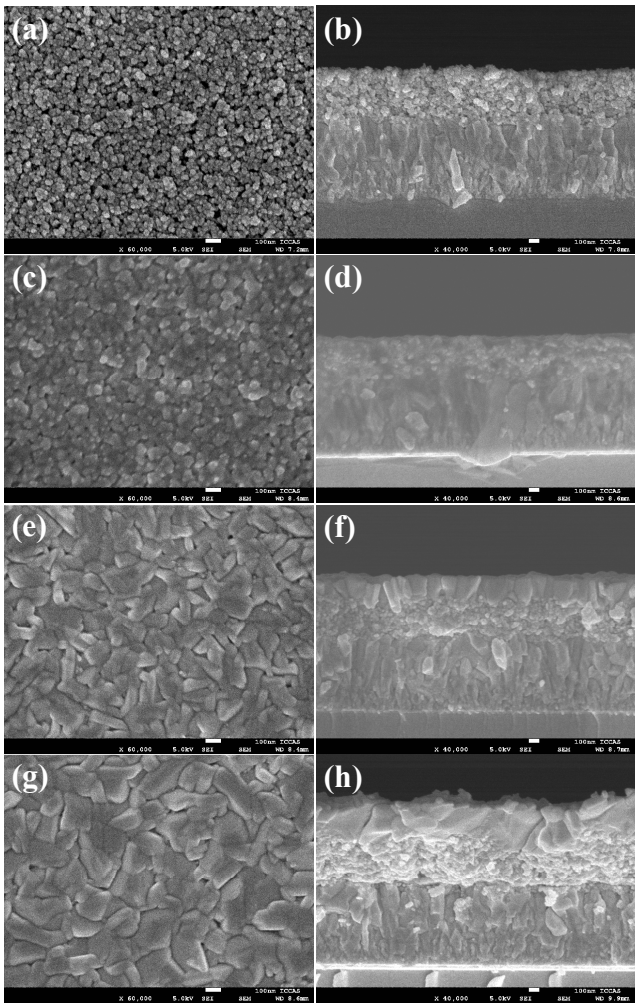

Fig.1 Top-view (a, c, e, g) and cross-sectional (b, d, f, h) SEM images of the mesoporous TiO_2 film (a, b), PbO coated TiO_2 film obtained by electrodeposition method (c, d), PbI_2 coated TiO_2 film obtained by in-situ conversion of PbO in iodine vapour (e, f), $CH_3NH_3PbI_3$ coated TiO_2 film obtained by reaction of PbI_2 with CH_3NH_3I (g, h).

For further investigation of the evolution, UV-vis absorption spectra and X-ray differaction (XRD) patterns were conducted for the deposition at different stages. As shown in **Figure 2a**, the absorption spectrum of the deposited PbO on TiO_2 film is in the visible short-wavelength region with absorption onset at ~520 nm, similar to that of the previous report.[22] After the iodination, the absorption spetrum is red-shifted with a typical absorption peak at 500 nm for PbI_2.[24] After the interdiffusion reaction between PbI_2 and MAI, the film shows the typical absorption spectrum of the perovskite with the onset at 770 nm. **Figure 2b** shows the XRD patterns of PbO, PbI_2 and $MAPbI_3$ on the TiO_2 films. For comparison, the XRD pattern of the bare TiO_2 films was recorded. After the PbO deposition, two aparent new peaks appeared at 28.3° and 32.4°. After the iodization, the two peaks disapeared,

and four new peaks appeared at 12.9°, 25.6°, 38.9°, and 53.2°, corresponding to the (001), (002), (003) and (004) lattice planes of the 2H polytype PbI_2 (hexagonal structure). After the interdiffusion reaction, new peaks appeared at 14.2, 20.1, 28.5, 31.9 and 40.7°, assigned to the (110), (112), (220), (310), and (224) planes of the tetragonal perovskite $CH_3NH_3PbI_3$. The results indicate the perovskite was successfully deposited on the porous TiO_2 film by the sequential deposition process starting from the electrodeposited PbO.

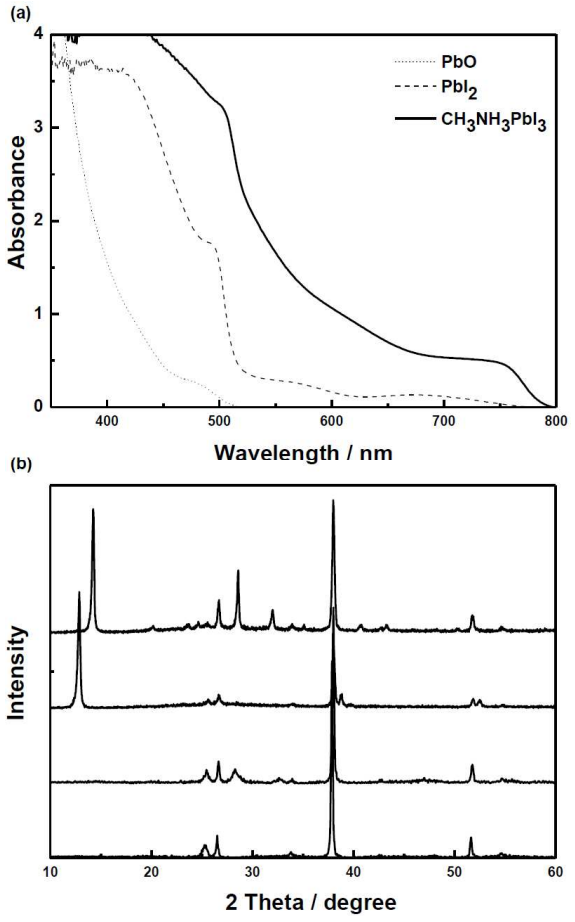

Fig. 2 Uv-vis spectra (a) and XRD diffraction paterns (b) of the PbO, PbI_2 and $CH_3NH_3PbI_3$ on the mesoporous TiO_2 film obtained by sequential deposition processes: electrodeposition, iodization and the interdiffusion reaction.

The in-situ formed perovskite films were used as photoanode in combination with a hole transport material and Au back electrode for the perovskite solar cell. The detailed fabrication process and characterization are described in the experimental section in the supporting information. Briefly, the FTO glass is coated with a compact layer of TiO_2 (~80 nm), then a mesoporous layer of TiO_2 (~350 nm). On the film, PbO was electrondeposited, followed by the iodination for PbI_2, and solid-solid or solid-liquid interdiffusion reaction with MAI. Then, spiro-MeOTAD (2,2′,7,7′-tetrakis(*N*,*N*-di-*p*-methoxyphenylamine)-9,9-spirobifluorene) was deposited as a hole transport layer, followed by evaporation of 80 nm thick Au as back electrode.

Two devices were fabricated for examining the photovoltaic performance, where solid-solid (PbI_2 layer and MAI layer) and solid-liquid (PbI_2 film immersed in isopropanol solution of MAI) interdiffusion reaction between the PbI_2 and MAI were carried out for **device 1** and **device 2**, respectively. In **Figure 3a**, we show the photocurrent density-voltage (*J-V*) curves measured under simulated AM 1.5 illumination. The most efficient **device 1** gave a short-circuit photocurrent density (J_{sc}) of 19.81 mA cm^{-2}, an open-circuit voltage (V_{oc}) of 0.91 V, and fill factor (*FF*) of 0.69 to yield an power conversion efficiency (*PCE*) of 12.5%, while the **device 2** having a J_{sc} of 18.86 mA cm^{-2}, a V_{oc} of 0.78 V, a *FF* of 0.61, and a *PCE* of 9.0%. The primary difference in the efficiency of both the devices is the low open-circuit voltage and fill fact of **device 2**, nearly 150 mV and 0.09 lower on average than those for **device 1**, as shown in **Table 1**. The low V_{oc} and *FF* of **device 2** would be ascribed to the highly rough perovskite upper layer on the TiO_2 film with poor surface coverage, leading to increased charge recombination. Thus, it seems that the solid-solid interdiffusion technique is benefit to the high-quality perovskite film and in turn high photovoltaic performance.[23]

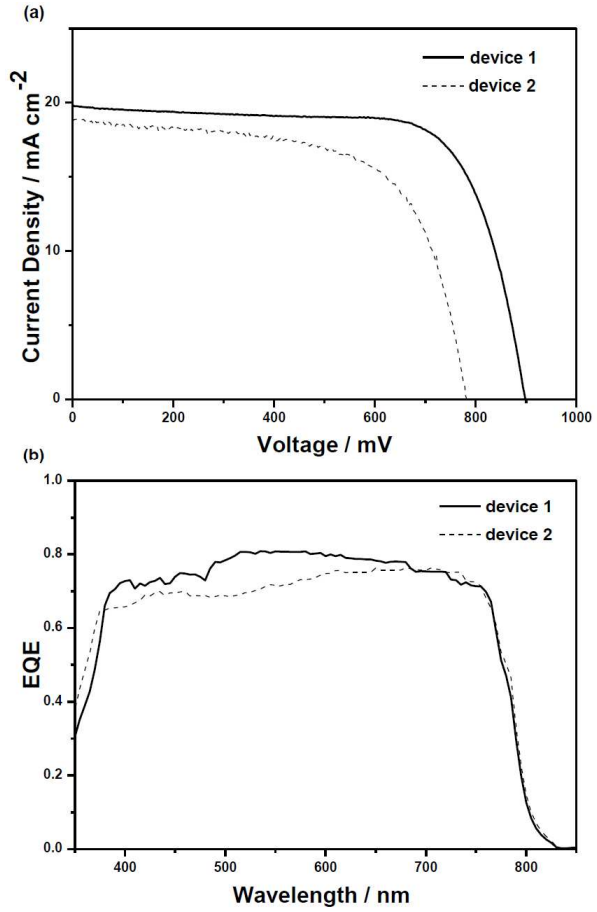

Fig. 3 *J-V* (a) and *EQE* (b) for **device 1** and **device 2**.

Figure 3b shows the external quantum efficiency (*EQE*) spectra of the two devices. Both the devices shows similar spectral sensitivity spanning from the visible to the near-IR (400 to 800 nm) with **device 2** showing slightly lower *EQE*, which is consistent with the measured short-circuit current density. Very recently, an in situ technique was reported for the preparation of the perovskite film, where thick (~6 μm) PbO/TiO_2 film was

employed. The film was prepared by spin-coating a mixture of TiO_2 colloid and PbI_2, followed by sintering at high temperature. [25] The resultant device gave a *PCE* of 8%, which is in contrast with the *PCE* of 12.5 % obtained here with a thin TiO_2 film (~350 nm). The results demonstrate that the electrodepositing PbO on mesoscopic TiO_2 film is a desirable approach for the fabrication of the perovskite solar cells. In addition, **device 1** exhibited high reproducibility with an average *PCE* of 11.3 ± 1.1%, as shown in **Table 1**.

Table 1. Photovoltaic performance of device 1 and device 2.

Device	J_{sc} / mA cm^{-2}	V_{oc} / mV	*FF*	*PCE* / %
device 1	19.81	910	0.69	12.5
a	18.73	884	0.66	11.3 ± 1.1[a]
device 2	18.86	780	0.61	9.0
	17.91	762	0.58	8.2 ± 1.7[a]

[a]The average and the standard deviation for the batch of 10 samples.

In the work reported here, the perovskite $CH_3NH_3PbI_3$ was in-situ deposited in the mesoscopic TiO_2 film starting from electrodepositing PbO, iodination for PbI_2, and interdiffusion reaction with MAI. It was found that the perovskite was well filled in the porous TiO_2 film with a dense and flat upper layer on the surface using this new technique. The as-prepared film was used as a light absorber for the perovskite solar cells, exhibiting a high *PCE* of 12.5% with high reproducibility. Moreover, this approach can afford large-scale production without the waste of Pb-containing materials encountered in the existing techniques. Thus, our finding open new routes for the fabrication of perovskite in mesoporous metal oxide film, and the technique is environmentally sound for the production of the perovskite mesoscopic solar cells at large scale. Further optimization of the device performance is now under investigation.

Acknowledgements

The authors greatly appreciate the financial support from the National Natural Science Foundation of China (Grant Nos. 21174149, 51173190, 21073203, 21076002 and 21121001), the National 863 Program (No. 2011AA050521), the 973 Program (2009CB930404, 2011CB932303, 2011CB808400), and the Scientific Equipment Program, ACS (YZ201106).

Notes and references

[a] *Key Laboratory of Green Printing, Institute of Chemistry, Chinese Academy of Sciences,Beijing, 100190, China*
E-mail: kjjiang@iccas.ac.cn, ylsong@iccas.ac.cn
[b] *School of Chemical Engineering and Technology, Tianjin University, Tianjin, 300072, China*
E-mail: zhouxueqin@tju.edu.cn.

† Electronic Supplementary Information (ESI) available: [details of any supplementary information available should be included here]. See DOI: 10.1039/b000000x/

1 A. Kojima, K. Teshima, Y. Shirai, T. Miyasaka, *J. Am. Chem. Soc.* 2009, **131**, 6050.
2 M. M. Lee, J. Teushcer, T. Miyasaka, T. N. Murakami, H. J. Snaith, *Science* 2012, **338**, 643.
3 H. S. Kim, C. R. Lee, J. H. Im, K. B. Lee, T. Moehl, A. Marchioro, S. J. Moon, R. Humphry-Baker, J. H. Yum, J. E. Moser, M. Grätzel, N. G. Park, *Sci. Rep.* 2012, **2**, 591.
4 L. Etgar, P. Gao , Z. Xue, Q , Peng , A. K. Chandiran, B. Liu , M. K. Nazeeruddin , M. Grätzel, *J. Am. Chem. Soc.* 2012, **134**, 17396.
5 J. H. Noh, S. H. Im, J. H. Heo, T. N. Mandal, S. I. Seok, *Nano Lett.* 2013, **13**, 1764.
6 J. H. Heo, S. H. Im, J. H. Noh, T. N. Mandal, C. S. Lim, J. A. Chang ,Y. H. Lee, H. J. Kim, A. Sarkar, M. K. Nazeeruddin, M. Grätzel, S. I. Seok, *Nature Photon.* 2013, **7**, 486.
7 J. Burschka, N. Pellet, S. J. Moon, R. Humphry-Baker, P. Gao, M. K. Nazeeruddin, M. Grätzel, *Nature* 2013, **499**, 316.
8 M. Liu, M. B. Johnston, H. J. Snaith, *Nature* 2013, **501**, 395.
9 J. H. Noh, S. H. Im, J. H. Heo, T. N. Mandal, S. I. Seok, *Nano Lett.* 2013, **13**, 1764.
10 J. M. Ball, M. M. Lee, A. Hey, H. Snaith, *Energy Environ. Sci.* 2013, **6**, 1739.
11 D. Liu, T. L. Kelly, *Nature Photon.* 2014*,* **8***, 133.*
12 Q. Chen, H. Zhou, Z. Hong, S. Luo, H. S. Duan, H. H. Wang, Y. Liu, G. Li, Y. Yang, *J. Am. Chem. Soc.* 2014, **136**, 622.
13 S. D. Stranks, G. E. Eperon, G. Grancini, C. Menelaou, M. J. P. Alcocer, T. Leijtens, L. M. Herz, A. Petrozza, H. J. Snaith, *Science* 2013, **342**, 341.
14 G. Xing, N. Mathews, S. Sun, S. S. Lim, Y. M. Lam, M. Grätzel, S. Mhaisalkar, T. C. Sum, *Science* 2013, **342**, 344.
15 A. Dualeh, N. Tétreault, T. Moehl, P. Gao, M. K. Nazeeruddin, M. Grätzel, *Adv. Func. Mater.* 2014, **24**, 3250.
16 A. K. Chandiran, A. Yella, M. T. Mayer, P. Gao, M. K. Nazeeruddin, M. Grätzel, *Adv. Mater.* DOI: 10.1002/adma.201306271.
17 K. Liang, D. B. Mitzi, M. T. Prikas, *Chem. Mater.* 1998, **10**, 403.
18 M. B. Sassin, C. N. Chervin, D. R. Rollison, J. W. Long, *Acc. Chem. Res.* 2013, **46**, 1062.
19 S. Sawatani, S. Ogawa, T. Yoshida, H. Minoura, *Adv. Func. Mater.* 2005, **15**, 297.
20 J. Qian, K.-J. Jiang, J.-H. Huang, Q.-S.g Liu, L.-M. Yang, Y. Song, *Angew. Chem. Int. Ed.* 2012, **51**, 10351.
21 I. Zhitomirsky, L. Gal-Or, A. Korn, H. W. Hennicke, *J. Mater. Sci. Lett.* 1995, **14**,807.
22 V. K. Dwivedi, J. J. Baumberg, G. V. Prakash, *Mater. Chem. Phys.* 2013, **137**, 941.
23 Z. Xiao, C. Bi, Y. Shao, Q. Dong, Q. Wang, Y. Yuan, C. Wang, Y. Gao, J. Huang, *Energy Environ. Sci.* 2014, **7**, 2619.
24 B. Conings, L. Baeten, C. D. Dobbelaere, J. Dhaen, J. Manca, H-G. Boyen, *Adv. Mater.* 2014, **26**, 2041.
25 Y. Xiao, J.-Y. Lin, S.-Y. Tai, S.-W. Chou, G. Yue, J. Wu, *J. Mater. Chem.* 2012, **22**, 19919.